Research Square

Preprints are preliminary reports that have not undergone peer review.
They should not be considered conclusive, used to inform clinical practice,
or referenced by the media as validated information.

14-3-3γ Knockdown Exacerbates $CoCl_2$-Induced Hypoxia-Like Injury in SH-SY5Y Cells by Enhancing Oxidative Stress and Apoptosis

Junli Liu

1fy2018008@xxmu.edu.cn

the First Affiliated Hospital of Henan Medical University

Yifan Zhang

the First Affiliated Hospital of Henan Medical University

Qiongya Si

the First Affiliated Hospital of Henan Medical University

Kehua Li

the First Affiliated Hospital of Henan Medical University

Jingnan Liu

the First Affiliated Hospital of Henan Medical University

Jianhua Zhao

the First Affiliated Hospital of Henan Medical University

Research Article

Keywords: YWHAG, 14-3-3γ, $CoCl_2$, SH-SY5Y, chemical hypoxia, oxidative stress, apoptosis

Posted Date: July 24th, 2026

DOI: https://doi.org/10.21203/rs.3.rs-10293511/v1

License: This work is licensed under a Creative Commons Attribution 4.0 International License.
Read Full License

Additional Declarations: No competing interests reported.

Abstract

Hypoxia-related neuronal injury is a major component of ischemic stroke. 14-3-3γ, encoded by *YWHAG*, participates in neuronal signaling and cellular stress responses, but its role in chemical hypoxia-like injury remains unclear. Here, SH-SY5Y cells were exposed to cobalt chloride ($CoCl_2$) to establish a hypoxia-like injury model, and *YWHAG* mRNA expression and function were examined by CCK-8 assay, quantitative real-time PCR, Western blotting, DCFH-DA staining, Annexin V-FITC/PI flow cytometry, and siRNA-mediated knockdown. $CoCl_2$ decreased cell viability in a concentration- and time-dependent manner. Exposure to 400 μM $CoCl_2$ for 24 h increased *YWHAG* mRNA and 14-3-3γ protein levels and activated apoptosis-related signaling. Under this condition, 14-3-3γ knockdown further increased reactive oxygen species accumulation, apoptosis, the Bax/Bcl-2 ratio, and cleaved caspase-3 expression. These findings indicate that 14-3-3γ is induced as an endogenous response to $CoCl_2$-triggered hypoxia-like stress and may mitigate oxidative stress and apoptosis in SH-SY5Y cells.

Simple Summary

A shortage of oxygen is a major cause of brain-cell damage during ischemic stroke. In this study, we used human neuron-like cells to test whether a protein called 14-3-3 gamma changes when cells are exposed to cobalt chloride, a chemical commonly used to mimic low-oxygen stress in the laboratory. We found that cobalt chloride reduced cell survival and increased oxidative damage and programmed cell death. The amount of 14-3-3 gamma also increased under these conditions. When we experimentally reduced this protein, cell damage became worse. These findings suggest that 14-3-3 gamma may help neuron-like cells resist low-oxygen-related stress. More work in models that better reflect stroke biology is needed before clinical relevance can be considered.

1. Introduction

Ischemic stroke interrupts cerebral blood supply and initiates local hypoxia, energy failure, oxidative stress, mitochondrial dysfunction, inflammation and regulated cell-death programs [1, 2]. Damage evolves across the neurovascular unit, where interactions among neurons, endothelial cells, glia and the extracellular matrix influence the progression of ischemic injury [3]. Although reperfusion-based therapies improve outcomes in selected patients, their use is limited by strict treatment windows and safety concerns [4]. Therefore, identifying endogenous molecular responses that influence neuronal survival under hypoxia-related stress remains important for understanding ischemic brain injury and for nominating candidate targets for further investigation.

Hypoxia-inducible factor-1α (HIF-1α) is a central transcriptional regulator of cellular adaptation to reduced oxygen availability [5, 6]. HIF-1α-dependent signaling regulates angiogenic and metabolic pathways, including vascular endothelial growth factor (VEGF), whereas excessive or prolonged hypoxic stress can exacerbate oxidative and apoptotic injury [7]. Cobalt chloride ($CoCl_2$) is widely used as a chemical hypoxia mimetic because it stabilizes HIF-1α and produces reproducible hypoxia-like cellular

responses [8, 9]. $CoCl_2$-induced models have been applied to neuronal and neuroblastoma-derived cells to study ROS generation, mitochondrial dysfunction, pyroptosis and apoptosis [10, 11]. SH-SY5Y cells are commonly used as a neuron-like in vitro model for neurotoxicity, ischemia/reperfusion-related injury and neuroprotective mechanisms [12].

The 14-3-3 protein family comprises highly conserved regulatory proteins that bind phosphorylated client proteins and participate in signal transduction, metabolism, cytoskeletal organization, cell-cycle regulation, apoptosis and stress responses [13, 14]. The γ isoform, encoded by YWHAG, is expressed in the nervous system and has been implicated in neurological disease [15, 16]. 14-3-3 proteins are also involved in brain development processes, including neurogenesis, neuronal migration and neuromorphogenesis [17]. Disease-oriented studies have further linked YWHAG/14-3-3γ to Parkinson's disease-related cognitive impairment and Alzheimer's disease-related cerebrospinal fluid proteomic signatures [18, 19].

Experimental evidence further suggests that 14-3-3γ contributes to neuronal and glial responses to ischemic or nutrient-deprivation stress. Selective 14-3-3γ induction has been associated with autophagic flux in starved neurons and with β-catenin/Bax-related neuronal survival during ischemia [20, 21]. In astrocytes and ischemia/reperfusion models, 14-3-3γ-related signaling has been linked to phosphorylated Bad and NF-κB regulation [22, 23]. YWHAG has also been implicated in a miRNA-mediated oxidative-stress pathway after cerebral ischemia/reperfusion injury [24]. However, the expression pattern and functional role of 14-3-3γ in $CoCl_2$-induced hypoxia-like injury in SH-SY5Y cells remain incompletely characterized.

Accordingly, we established a $CoCl_2$-induced hypoxia-like injury model in SH-SY5Y cells to determine whether $CoCl_2$ alters YWHAG/14-3-3γ expression and whether siRNA-mediated knockdown modulates oxidative stress and apoptosis. We hypothesized that 14-3-3γ is induced as an adaptive response to hypoxia-like stress and that its depletion exacerbates $CoCl_2$-induced injury.

2. Materials and Methods

2.1. Cell Culture

Human SH-SY5Y cells were obtained from the Cell Bank of the Chinese Academy of Sciences (Shanghai, China). Cells were cultured in high-glucose DMEM supplemented with 10% fetal bovine serum and 1% penicillin-streptomycin in a humidified incubator at 37°C with 5% CO_2. Cells in the logarithmic growth phase were used for experiments.

2.2. Reagents and Antibodies

$CoCl_2$ (Sigma-Aldrich, St. Louis, MO, USA; Cat. No. 904104), Cell Counting Kit-8 (Dojindo, Kumamoto, Japan; Cat. No. MC0301-1500), ROS Assay Kit (Kaiji Biotechnology, Nanjing, China; Cat. No. KGA7308-100), Annexin V-FITC/PI Apoptosis Detection Kit (Kaiji Biotechnology; Cat. No. KGA1102-100),

Lipofectamine 3000 (Thermo Fisher Scientific, Waltham, MA, USA; Cat. No. BMU111-CN), YWHAG-targeting siRNAs (MedChemExpress, Monmouth Junction, NJ, USA; Cat. No. No.HY-RS15942) were used in this study. Primary antibodies against 14-3-3γ (Proteintech Wuhan, China; Cat. No.12381-1-AP), Bax (Abways, Shanghai, China; Cat. Nos. CY5059), Bcl-2 (Abways; Cat. No. CY5582), cleaved caspase-3 (Abways; Cat. No. CY5501), and β-actin (Abways; Cat. No. AB0035) were used in this study. Detailed information regarding host species and working dilutions is provided in Table S1.

2.3. CCK-8 Cell Viability Assay

SH-SY5Y cells were seeded into 96-well plates at approximately 8,000–10,000 cells per well. Cells were treated with 0, 100, 200, 300, 400, 500, 600, 700 or 800 μM $CoCl_2$ for 24, 36 or 48 h. Each group included five technical replicate wells, and the assay was repeated in independent experiments. After treatment, 10 μL of CCK-8 solution was added to each well and incubated for 1 h. Absorbance was measured at 450 nm using a microplate reader. Cell viability was expressed as a percentage of the untreated control group.

2.4. Quantitative Real-Time PCR

Total RNA was extracted using TRIzol reagent and reverse-transcribed using NovoScript® Plus All-in-one 1st Strand cDNA Synthesis SuperMix (gDNA Purge) (Novoprotein, Shanghai, China; Cat. No. E047-01A). Quantitative PCR was performed on a QuantStudio 5 (Life Technologies, Singapore) using NovoStart® SYBR qPCR SuperMix Plus (Novoprotein, Shanghai, China; Cat. No. E096-01A) under the following cycling conditions: 95°C for 1 min; 40 cycles of 95°C for 20 s and 60°C for 1 min. Relative YWHAG mRNA expression was calculated using the $2^{-\Delta\Delta Ct}$ method with ACTB as the internal control [25]. The primer sequences are listed in Table 1.

Table 1
Primer sequences used for qRT-PCR.

Primer	Sequence
14-3-3γ-F	5'-CCATTCGTTTAGGTCTTGCTCTCA-3'
14-3-3γ-R	5'-TCTTCACTCAGCGTGTCCAGTTC-3'
β-actin-F	5'-GGCTCTTTTCCAGCCTTCCT-3'
β-actin-R	5'-AATGCCAGGGTACATGGTGG-3'

2.5. Western Blotting

Total protein was extracted using RIPA lysis buffer supplemented with protease and phosphatase inhibitors. Protein concentration was determined using a BCA protein assay kit according to the manufacturer's instructions. Equal amounts of protein were separated by SDS-PAGE and transferred onto PVDF membranes. Membranes were blocked with 5% non-fat milk and incubated overnight at 4°C with primary antibodies against 14-3-3γ, Bax, Bcl-2, cleaved caspase-3 and β-actin. After incubation with HRP-

conjugated secondary antibodies, protein bands were visualized using enhanced chemiluminescence. Band intensities were quantified using ImageJ and normalized to β-actin.

2.6. siRNA Transfection

Three 14-3-3γ-specific siRNA sequences and a negative-control siRNA were used to evaluate knockdown efficiency. SH-SY5Y cells were seeded into 24-well plates and transfected at approximately 80% confluence. siRNA and Lipofectamine 3000 were diluted in serum-free medium, mixed and incubated for 15–30 min to form transfection complexes. After 6–8 h of transfection, the medium was replaced with complete culture medium. FAM-labeled negative-control siRNA was used to assess transfection efficiency by fluorescence microscopy. The final optimized siRNA concentration was 200 nM, and si-14-3-3γ-3 was selected for subsequent experiments based on the strongest protein-level knockdown.

2.7. ROS Detection

Intracellular ROS levels were measured using a DCFH-DA fluorescence probe. After treatment, cells were incubated with DCFH-DA working solution diluted 1:1000 in serum-free medium for 20 min at 37°C. Cells were washed to remove extracellular probe, counterstained with DAPI where appropriate, and imaged using a Leica DMI4000B inverted fluorescence microscope (Leica Microsystems, Wetzlar, Germany). Fluorescence intensity was quantified using ImageJ.

2.8. Annexin V-FITC/PI Apoptosis Assay

Cell apoptosis was detected using an Annexin V-FITC/PI apoptosis detection kit. After treatment, cells were harvested using EDTA-free trypsin, resuspended in binding buffer and incubated with Annexin V-FITC and propidium iodide for 15 min in the dark. Apoptotic cells were detected by BD FACSCalibur flow cytometer (Becton Dickinson, Franklin Lakes, NJ, USA). The total apoptosis rate was calculated as the sum of early and late apoptotic cells.

2.9. Statistical Analysis

All experiments were performed using at least three independent biological replicates. Data are presented as mean ± SD. Two-group comparisons were analyzed using an unpaired two-tailed Student's t-test. Multiple-group comparisons were analyzed using one-way ANOVA followed by Tukey's post hoc test. Statistical analyses were performed in GraphPad Prism version X.X (GraphPad Software, San Diego, CA, USA), and $p < 0.05$ was considered statistically significant. The exact n values are provided in the figure legends.

3. Results

3.1. $CoCl_2$ Reduced SH-SY5Y Cell Viability in a Concentration- and Time-Dependent Manner

CCK-8 assays showed that $CoCl_2$ reduced SH-SY5Y cell viability in a concentration- and time-dependent manner. At 24 h, 100 and 200 μM $CoCl_2$ did not significantly suppress viability, whereas higher concentrations progressively reduced cell viability. At 500 μM, cell viability decreased to approximately 72%, and at 800 μM it decreased to approximately 50%. At 36 and 48 h, the cytotoxic effect was more pronounced. Based on the viability data, 0–500 μM $CoCl_2$ was used for expression screening, and 400 μM $CoCl_2$ for 24 h was selected for subsequent mechanistic experiments because it produced clear injury while preserving sufficient viable cells(Figure.1).

3.2. $CoCl_2$ Upregulated 14-3-3γ mRNA Expression in SH-SY5Y Cells

qRT-PCR analysis showed that 14-3-3γ mRNA levels increased as the $CoCl_2$ concentration increased. Compared with the 0 μM control group, 100, 200 and 300 μM $CoCl_2$ did not significantly change 14-3-3γ mRNA expression. However, 400 μM $CoCl_2$ significantly increased 14-3-3γ mRNA expression at 24, 36 and 48 h, indicating that chemical hypoxia-like stress upregulated 14-3-3γ transcription in SH-SY5Y cells(Figure.2).

3.3. $CoCl_2$ Increased 14-3-3γ Protein Expression

Western blot analysis further confirmed the increase in 14-3-3γ at the protein level. After treatment with 400 μM $CoCl_2$, 14-3-3γ protein expression was significantly increased at 24, 36 and 48 h compared with untreated controls. The strongest induction was observed at 24 h. Therefore, 400 μM $CoCl_2$ for 24 h was used in subsequent functional experiments(Figure.3).

3.4. $CoCl_2$ Induced Apoptosis-Related Protein Changes

Western blotting showed that $CoCl_2$ treatment increased the expression of the pro-apoptotic proteins Bax and cleaved caspase-3 and decreased the expression of the anti-apoptotic protein Bcl-2. These changes indicate that $CoCl_2$-induced chemical hypoxia-like stress activated apoptosis-related signaling in SH-SY5Y cells(Figure.4).

3.5. siRNA Transfection Downregulated 14-3-3γ Protein Expression

FAM-labeled siRNA produced visible green fluorescence in the cytoplasm after transfection, indicating successful siRNA delivery into SH-SY5Y cells. qRT-PCR showed no statistically significant reduction in 14-3-3γ mRNA at 24 or 48 h after transfection, whereas Western blotting showed that si-14-3-3γ-3 significantly reduced 14-3-3γ protein expression. Therefore, si-14-3-3γ-3 was selected for functional assays(Figure.5).

3.6. 14-3-3γ Knockdown Aggravated $CoCl_2$-Induced Apoptosis

Flow cytometry showed that $CoCl_2$ treatment significantly increased the apoptosis rate from approximately 8% in control cells to approximately 33%. 14-3-3γ knockdown further increased the apoptosis rate to approximately 40%, which was significantly higher than that in the $CoCl_2$ group. Compared with the $CoCl_2$ group, the $CoCl_2$ + si-YWHAG group showed a significantly higher total apoptosis rate, indicating that YWHAG knockdown aggravated $CoCl_2$-induced apoptotic injury(Figure.6).

3.7. 14-3-3γ Knockdown Enhanced ROS Accumulation under $CoCl_2$-Induced Stress

DCFH-DA fluorescence staining showed that $CoCl_2$ treatment increased intracellular ROS levels. ROS accumulation was further enhanced after 14-3-3γ knockdown, suggesting that endogenous 14-3-3γ may contribute to the suppression of oxidative stress during $CoCl_2$-induced injury(Figure.7).

3.8. 14-3-3γ Knockdown Activated Apoptosis-Related Signaling

Western blotting showed that $CoCl_2$ increased 14-3-3γ expression and elevated the Bax/Bcl-2 ratio. 14-3-3γ knockdown attenuated the $CoCl_2$-induced increase in 14-3-3γ, further increased the Bax/Bcl-2 ratio and significantly increased cleaved caspase-3 expression. Under $CoCl_2$ exposure, YWHAG knockdown increased ROS accumulation, the Bax/Bcl-2 ratio, and cleaved caspase-3 expression, consistent with enhanced oxidative stress and activation of mitochondrial apoptosis-related signaling(Figure.8).

Table 2
Summary of model optimization and functional outcomes.

Experiment	Condition	Key outcome
CCK-8 screening	0–800 μM $CoCl_2$; 24, 36 and 48 h	Concentration- and time-dependent decrease in viability
Expression screening	0–500 μM $CoCl_2$; 24, 36 and 48 h	14-3-3γ mRNA increased at 400 μM
Optimized model	400 μM $CoCl_2$ for 24 h	Robust 14-3-3γ protein induction with sufficient viable cells
Functional assay	$CoCl_2$ + si-14-3-3γ-3	Enhanced ROS accumulation and apoptosis

4. Discussion

In this study, we established a $CoCl_2$-induced chemical hypoxia-like injury model in SH-SY5Y cells and investigated the expression and functional significance of 14-3-3γ. The main findings were as follows: $CoCl_2$ reduced SH-SY5Y cell viability in a concentration- and time-dependent manner; 400 μM $CoCl_2$ upregulated 14-3-3γ mRNA and protein expression; $CoCl_2$ increased ROS accumulation and apoptosis-related signaling; and siRNA-mediated 14-3-3γ knockdown further aggravated ROS accumulation, apoptosis rate, Bax/Bcl-2 imbalance and cleaved caspase-3 activation. These results support the

interpretation that 14-3-3γ is upregulated as an endogenous stress-response protein and may protect neuron-like cells from $CoCl_2$-induced oxidative and apoptotic injury. This interpretation is consistent with reports showing 14-3-3γ induction during ischemic neuronal and astrocytic stress responses [21, 22].

$CoCl_2$ is commonly used to mimic chemical hypoxia because it stabilizes HIF-1α and reproduces cellular responses associated with oxygen deprivation [8]. In the present study, SH-SY5Y cell viability decreased progressively with increasing $CoCl_2$ concentration and longer treatment duration, which is consistent with the expected cytotoxic profile of chemical hypoxia-like models. Previous $CoCl_2$-based SH-SY5Y studies have also reported neurodegenerative or stress-related cellular injury under chemical hypoxia-like conditions [10]. The selection of 400 μM $CoCl_2$ for 24 h provided a balance between a measurable stress response and sufficient cell survival for knockdown experiments. Nevertheless, $CoCl_2$ models do not fully reproduce oxygen-glucose deprivation or the complex cellular interactions that occur during in vivo ischemic stroke.

Hypoxia-related stress is a central component of ischemic brain injury [1]. During ischemia, impaired oxygen utilization and mitochondrial dysfunction can increase ROS generation, which damages lipids, proteins, DNA and organelles and contributes to apoptotic signaling [2]. In this model, $CoCl_2$ increased ROS fluorescence and shifted apoptosis-related protein expression toward a pro-apoptotic pattern, including increased Bax, decreased Bcl-2 and increased cleaved caspase-3. These findings support the suitability of the model for studying mechanisms related to hypoxia-like oxidative stress and apoptosis in neuron-like cells.

The upregulation of 14-3-3γ after $CoCl_2$ exposure is a key observation. 14-3-3 proteins function as regulatory hubs that bind phosphorylated client proteins and modulate survival, stress response, metabolism and apoptosis [13]. In the nervous system, 14-3-3 isoforms participate in neuronal development and neurological disease [26]. The γ isoform has received increasing attention because it is implicated in brain disorders and stress-related neuronal responses [15]. Selective 14-3-3γ induction has been associated with Beclin-1-LC3 autophagic flux in starved neurons [20]. Ischemic cortical neuron studies further support a relationship between 14-3-3γ, β-catenin/Bax signaling and cell survival [21]. In line with previous reports in neuronal and glial injury models, our data indicate that $CoCl_2$ increases 14-3-3γ expression in SH-SY5Y cells. This suggests that 14-3-3γ may be part of an adaptive cellular response to hypoxia-like stress.

The knockdown experiments further support a protective role for endogenous 14-3-3γ. After si-14-3-3γ treatment, $CoCl_2$-induced apoptosis increased from approximately 33% to approximately 40%, accompanied by greater ROS accumulation, an elevated Bax/Bcl-2 ratio and increased cleaved caspase-3 expression. Bax promotes mitochondrial outer membrane permeabilization, whereas Bcl-2 counteracts apoptotic signaling; therefore, an increased Bax/Bcl-2 ratio indicates a shift toward mitochondrial apoptosis [2]. Cleaved caspase-3 is a major executioner of apoptotic cell death. Previous ischemic neuronal and astrocytic studies linking 14-3-3γ to β-catenin/Bax or phosphorylated Bad provide a mechanistic context for this phenotype [21, 22]. The enhancement of these markers after 14-3-3γ

knockdown indicates that endogenous 14-3-3γ restrains apoptosis-related signaling under $CoCl_2$-induced stress.

One possible explanation is that 14-3-3γ modulates mitochondrial and oxidative-stress pathways. Previous studies have linked 14-3-3γ to β-catenin/Bax signaling in ischemic cortical neurons [27]. In ischemic astrocytes, 14-3-3γ association with phosphorylated Bad has been reported to attenuate cellular injury [22]. Other work indicates that 14-3-3 isoforms can differentially regulate NF-κB signaling after cerebral ischemia/reperfusion [23]. A lncRNA/miR-30a-5p/YWHAG pathway has also been associated with apoptosis, oxidative stress and inflammation after cerebral ischemia/reperfusion injury [24]. In astrocytes, ischemia-induced 14-3-3γ upregulation involves the JNK/c-Jun/AP-1 pathway [28]. Hydrogen peroxide preconditioning in PC12 cells has been associated with MAPK-dependent upregulation of 14-3-3 proteins [29]. Therefore, 14-3-3γ knockdown may weaken endogenous anti-oxidative or anti-apoptotic defenses, leading to greater ROS accumulation and activation of mitochondrial apoptosis. However, the present study did not directly assess mitochondrial membrane potential, antioxidant enzyme activity, HIF-1α, NF-κB, JNK, ERK1/2, p38 MAPK or autophagy markers, so the precise downstream mechanism remains to be determined.

The discrepancy between qRT-PCR and Western blot findings after siRNA transfection also deserves attention. siRNA-mediated RNA interference is a post-transcriptional gene-silencing approach, and its apparent effects can vary with sequence, dose, sampling time and the relative stability of target mRNA and protein [30]. A discrepancy between qRT-PCR and Western blotting was observed after siRNA transfection. This may reflect differences in mRNA turnover, protein stability, transfection efficiency, or the timing of sample collection. Because only one siRNA was advanced to downstream experiments and no rescue assay was performed, off-target effects cannot be excluded.

Several limitations should be acknowledged. First, $CoCl_2$ is a chemical hypoxia mimetic and does not fully recapitulate oxygen-glucose deprivation or in vivo ischemic stroke. Second, only SH-SY5Y cells were examined, which limits biological generalizability. Third, rescue or overexpression experiments are needed to strengthen causal inference. Fourth, direct model-validation markers, such as HIF-1α stabilization, were not assessed.

Despite these limitations, the present study provides evidence that 14-3-3γ is upregulated in $CoCl_2$-induced SH-SY5Y cells and that its knockdown aggravates oxidative stress and apoptosis. Together with prior ischemic neuron and astrocyte studies, these findings support the hypothesis that 14-3-3γ functions as an endogenous protective factor under chemical hypoxia-like stress and should be investigated further in more physiologically relevant models of ischemic neuronal injury [22, 27].

5. Conclusions

In summary, $CoCl_2$-induced hypoxia-like stress increased YWHAG/14-3-3γ expression in SH-SY5Y cells, and 14-3-3γ knockdown exacerbated oxidative stress and apoptosis. These findings support a protective association for endogenous 14-3-3γ in this chemical hypoxia-like model. However, rescue experiments

and validation in oxygen-glucose deprivation systems, primary neuronal cultures, and in vivo stroke models are required before broader mechanistic or translational conclusions can be drawn.

Declarations

Author Contributions

Junli Liu ang Yifan Zhang drafted the manuscript and conceptualization and supervision.. Jingnan Liu and Kehua Li prepared the figures and the tables. Jianhua Zhao supervised the manuscript. All authors contributed to study conception and design, commented on previous versions of the manuscript, and read and approved the final manuscript.

Funding

This work was supported by the Henan Natural Science Foundation Project (No. 262300420548), the Henan Medical Researcher Overseas Training Program (No. HNMOTO2025081), the Henan High-level Talent International Training Project (No. GCC2026048), the Key Scientific Research Project Plan of Higher Education Institutions in Henan Province (No. 25A320037), and the Henan Provincial Health Commission (No. LHGJ20190457). The funders had no role in study design, data collection, data interpretation, manuscript preparation or the decision to publish.

Institutional Review Board Statement

Not applicable.

Informed Consent Statement

Not applicable.

Data Availability Statement

The original data presented in this study are openly available in [repository name] at [DOI/accession number]. Uncropped Western blot images, densitometry data, and raw flow-cytometry files are provided in the Supplementary Materials.

Acknowledgments

Not applicable.

Conflicts of Interest

The authors declare no conflict of interest.

Clinical trial number

not applicable.

References

1. Qin C, Yang S, Chu Y-H, Zhang H, Pang X-W, Chen L, Zhou L-Q, Chen M, Tian D-S, Wang W (2022) Signaling Pathways Involved in Ischemic Stroke: Molecular Mechanisms and Therapeutic Interventions. Sig Transduct Target Ther 7:215. 10.1038/s41392-022-01064-1
2. Li H, Chen G (2022) Letter to Cell Death Pathways in Ischemic Stroke and Targeted Pharmacotherapy. Transl Stroke Res 13:357–358. 10.1007/s12975-021-00965-7
3. Wang L, Xiong X, Zhang L, Shen J (2021) Neurovascular Unit: A Critical Role in Ischemic Stroke. CNS Neurosci Ther 27:7–16. 10.1111/cns.13561
4. Jia J, Jiao W, Wang G, Wu J, Huang Z, Zhang Y (2024) Drugs/Agents for the Treatment of Ischemic Stroke: Advances and Perspectives. Med Res Rev 44:975–1012. 10.1002/med.22009
5. Zhang J, Han J, Li N, Zhou W (2025) Deciphering the Protective Role of HIF-1α Downregulation on HIBD through the MALAT1/miR-140-5p/TGFBR1/NF-κB Signaling Pathway. Mol Neurobiol 62:3343–3360. 10.1007/s12035-024-04451-7
6. Shen X, Li M, Wang C, Liu Z, Wu K, Wang A, Bi C, Lu S, Long H, Zhu G (2022) Hypoxia Is Fine-Tuned by Hif-1α and Regulates Mesendoderm Differentiation through the Wnt/β-Catenin Pathway. BMC Biol 20:219. 10.1186/s12915-022-01423-y
7. Choi Y, Kim J-S, Moon C, Baik J-H, Lee H-J, Son Y (2025) Transcriptional Profiling Uncovers Microglial HIF-1α Signaling as a Therapeutic Target of Radiation-Induced Brain Injury. Free Radic Biol Med 239:552–564. 10.1016/j.freeradbiomed.2025.08.014
8. Muñoz-Sánchez J, Chánez-Cárdenas ME (2019) The Use of Cobalt Chloride as a Chemical Hypoxia Model. J Appl Toxicol 39:556–570. 10.1002/jat.3749
9. Rana NK, Singh P, Koch B (2019) CoCl2 Simulated Hypoxia Induce Cell Proliferation and Alter the Expression Pattern of Hypoxia Associated Genes Involved in Angiogenesis and Apoptosis. Biol Res 52:12. 10.1186/s40659-019-0221-z
10. Guo Z, Tang J, Wang J, Zheng F, Zhang C, Wang Y-L, Cai P, Shao W, Yu G, Wu S et al (2021) The Negative Role of Histone Acetylation in Cobalt Chloride-Induced Neurodegenerative Damages in SHSY5Y Cells. Ecotoxicol Environ Saf 209:111832. 10.1016/j.ecoenv.2020.111832
11. Park CH, Park JY, Cho WG (2024) Chemical Hypoxia Induces Pyroptosis in Neuronal Cells by Caspase-Dependent Gasdermin Activation. *IJMS 25*, 2185. 10.3390/ijms25042185
12. Sang Q, Liu X, Wang L, Qi L, Sun W, Wang W, Sun Y, Zhang H (2018) Curcumin Protects an SH-SY5Y Cell Model of Parkinson's Disease Against Toxic Injury by Regulating HSP90. Cell Physiol Biochem 51:681–691. 10.1159/000495326
13. Segal D, Maier S, Mastromarco GJ, Qian WW, Nabeel-Shah S, Lee H, Moore G, Lacoste J, Larsen B, Lin Z-Y et al (2023) A Central Chaperone-like Role for 14-3-3 Proteins in Human Cells. Mol Cell 83:974–993e15. 10.1016/j.molcel.2023.02.018

14. Liu J, Cao S, Ding G, Wang B, Li Y, Zhao Y, Shao Q, Feng J, Liu S, Qin L et al (2021) The Role of 14-3-3 Proteins in Cell Signalling Pathways and Virus Infection. J Cell Mol Medi 25:4173–4182. 10.1111/jcmm.16490
15. Cho E, Park J-Y (2020) Emerging Roles of 14-3-3γ in the Brain Disorder. BMB Rep 53:500–511. 10.5483/BMBRep.2020.53.10.158
16. Foote M, Zhou Y 14-3-3 Proteins in Neurological Disorders
17. Cornell B, Toyo-oka K (2017) 14-3-3 Proteins in Brain Development: Neurogenesis, Neuronal Migration and Neuromorphogenesis. Front Mol Neurosci 10:318. 10.3389/fnmol.2017.00318
18. Peng Y, Zhu L, Bai Q, Wang L, Li Q (2024) Serum Level of YWHAG as a Diagnostic Marker of Cognitive Impairment in Parkinson's Disease Patients. Acta Neurol Belg 124:879–885. 10.1007/s13760-023-02441-5
19. Guo Y, Chen S-D, You J, Huang S-Y, Chen Y-L, Zhang Y, Wang L-B, He X-Y, Deng Y-T, Zhang Y-R et al (2024) Multiplex Cerebrospinal Fluid Proteomics Identifies Biomarkers for Diagnosis and Prediction of Alzheimer's Disease. Nat Hum Behav 8:2047–2066. 10.1038/s41562-024-01924-6
20. Xiong XX, Hu DX, Xu L, Lin H, Zhang Y, Li CY, Chen XQ (2019) Selective 14-3-3γ Upregulation Promotes Beclin-1-LC3-Autophagic Influx via β-Catenin Interaction in Starved Neurons In Vitro and In Vivo. Neurochem Res 44:849–858. 10.1007/s11064-019-02717-4
21. Guo T, Chen M, Liu J, Wei Z, Yuan J, Wu W, Wu Z, Lai Y, Zhao Z, Chen H et al (2023) Neuropilin-1 Promotes Mitochondrial Structural Repair and Functional Recovery in Rats with Cerebral Ischemia. J Transl Med 21:297. 10.1186/s12967-023-04125-3
22. Chen XQ, Fung Y-WW, Yu ACH (2005) Association of 14-3-3γ and Phosphorylated Bad Attenuates Injury in Ischemic Astrocytes. J Cereb Blood Flow Metab 25:338–347. 10.1038/sj.jcbfm.9600032
23. Hu C, Zhang S, Chen Q, Wang R (2022) Ovatodiolide Protects Ischemia-Reperfusion-Induced Neuronal Injury via Microglial Neuroinflammation via Mediating SIRT1/NF-κB Pathway. Brain Res Bull 180:97–107. 10.1016/j.brainresbull.2021.12.010
24. Zhou X, Wang Z, Xu B, Ji N, Meng P, Gu L, Li Y (2021) Long Non-Coding RNA NORAD Protects against Cerebral Ischemia/Reperfusion Injury Induced Brain Damage, Cell Apoptosis, Oxidative Stress and Inflammation by Regulating miR-30a-5p/YWHAG. Bioengineered 12:9174–9188. 10.1080/21655979.2021.1995115
25. Livak KJ, Schmittgen TD (2001) Analysis of Relative Gene Expression Data Using Real-Time Quantitative PCR and the 2 – ΔΔCT Method. Methods 25:402–408. 10.1006/meth.2001.1262
26. Vilmont V, Nowakowski RS, Zhou Y (2025) Role of the YWHAG Gene Mutations in Developmental and Epileptic Encephalopathy. Front Neurosci 19:1641250. 10.3389/fnins.2025.1641250
27. Lai XJ, Ye SQ, Zheng L, Li L, Liu QR, Yu SB, Pang Y, Jin S, Li Q, Yu ACH et al (2014) Selective 14-3-3γ Induction Quenches p-β-Catenin Ser37/Bax-Enhanced Cell Death in Cerebral Cortical Neurons during Ischemia. Cell Death Dis 5:e1184–e1184. 10.1038/cddis.2014.152
28. Hirayama Y, Le HPN, Hashimoto H, Ishii I, Koizumi S, Anzai N (2024) Preconditioning-Induced Facilitation of Lactate Release from Astrocytes Is Essential for Brain Ischemic Tolerance. *eNeuro 11*,

ENEURO.0494-23.2024. 10.1523/ENEURO.0494-23.2024

29. Mukherjee S, Roy S, Mukherjee S, Harikishore A, Bhunia A, Mandal AK (2024) 14-3-3 Interaction with Phosphodiesterase 8A Sustains PKA Signaling and Downregulates the MAPK Pathway. J Biol Chem 300:105725. 10.1016/j.jbc.2024.105725
30. Gangopadhyay S, Sharma SN, Das G, Ghosh A, Dilnawaj Y, Mukherjee M, Sinha S, R.Gore K (2026) Enhancing RNAi Activity through 4'-O-Hexadecyl-2'-Deoxythymidine Modification in the Passenger Strand. Bioorg Med Chem 137:118614. 10.1016/j.bmc.2026.118614

Figures

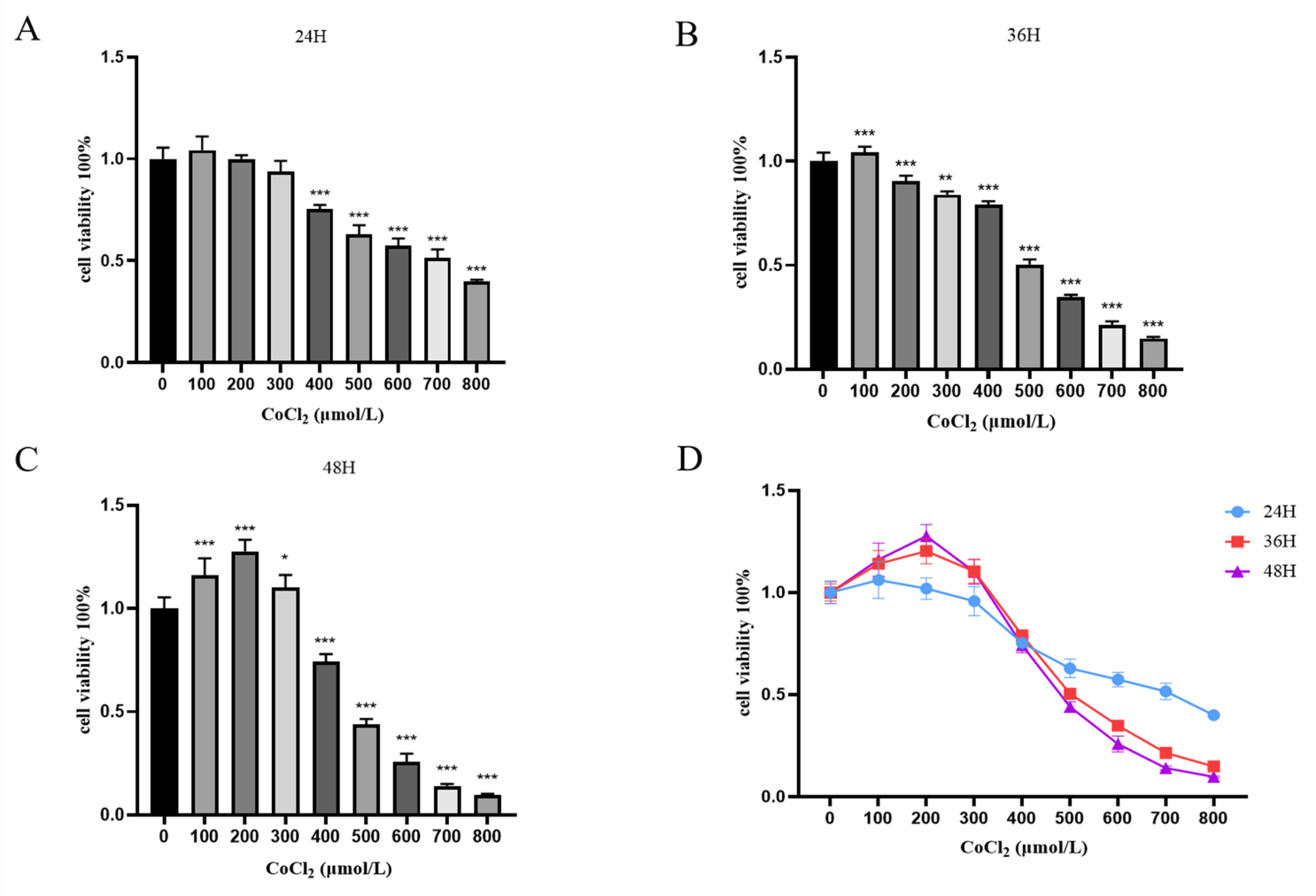


Figure 1

CCK-8 assay showing the effects of different concentrations of $CoCl_2$ on SH-SY5Y cell viability at 24, 36 and 48 h.

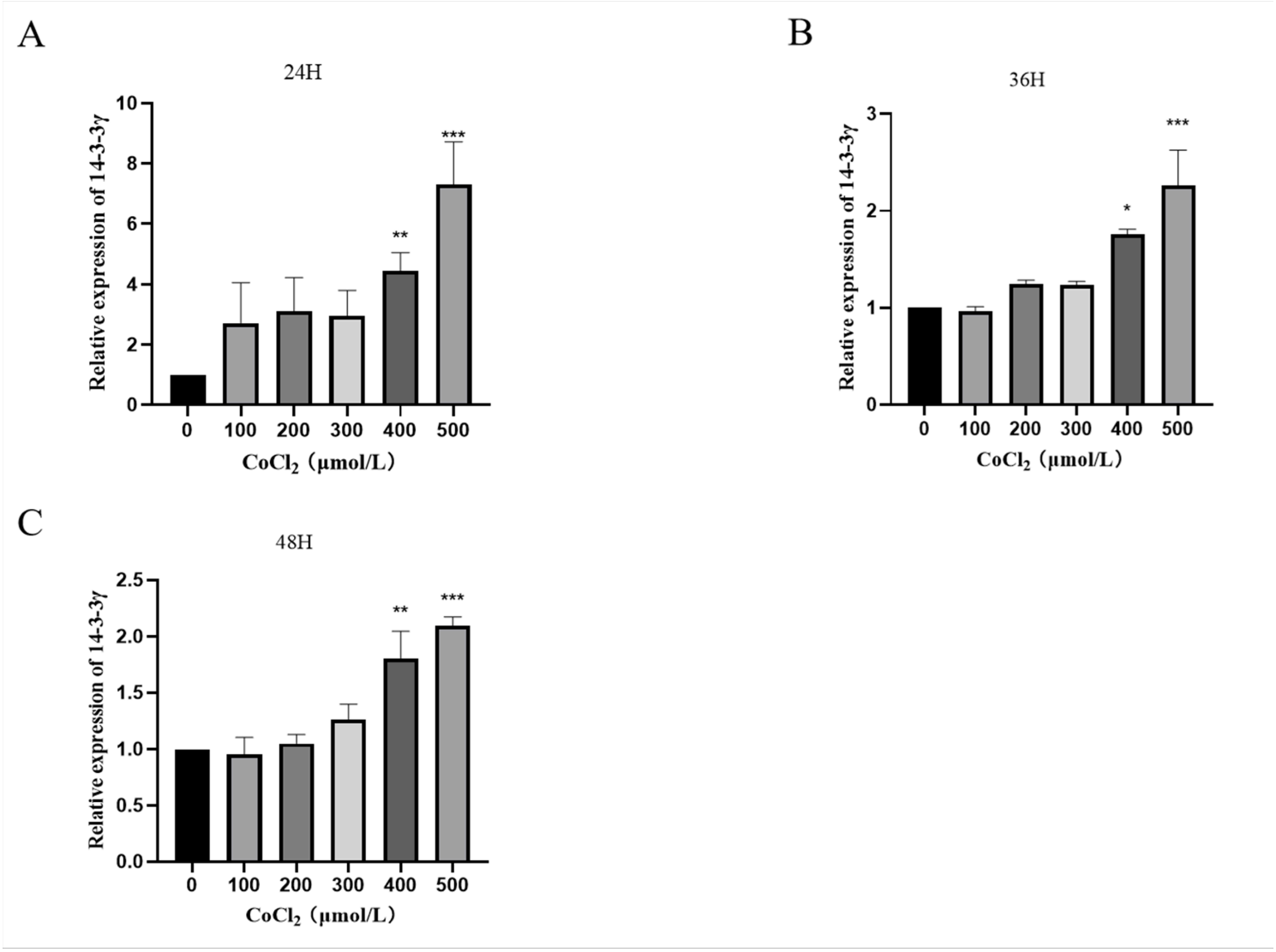


Figure 2

qRT-PCR analysis of 14-3-3γ mRNA expression after $CoCl_2$ treatment at different concentrations and time points.

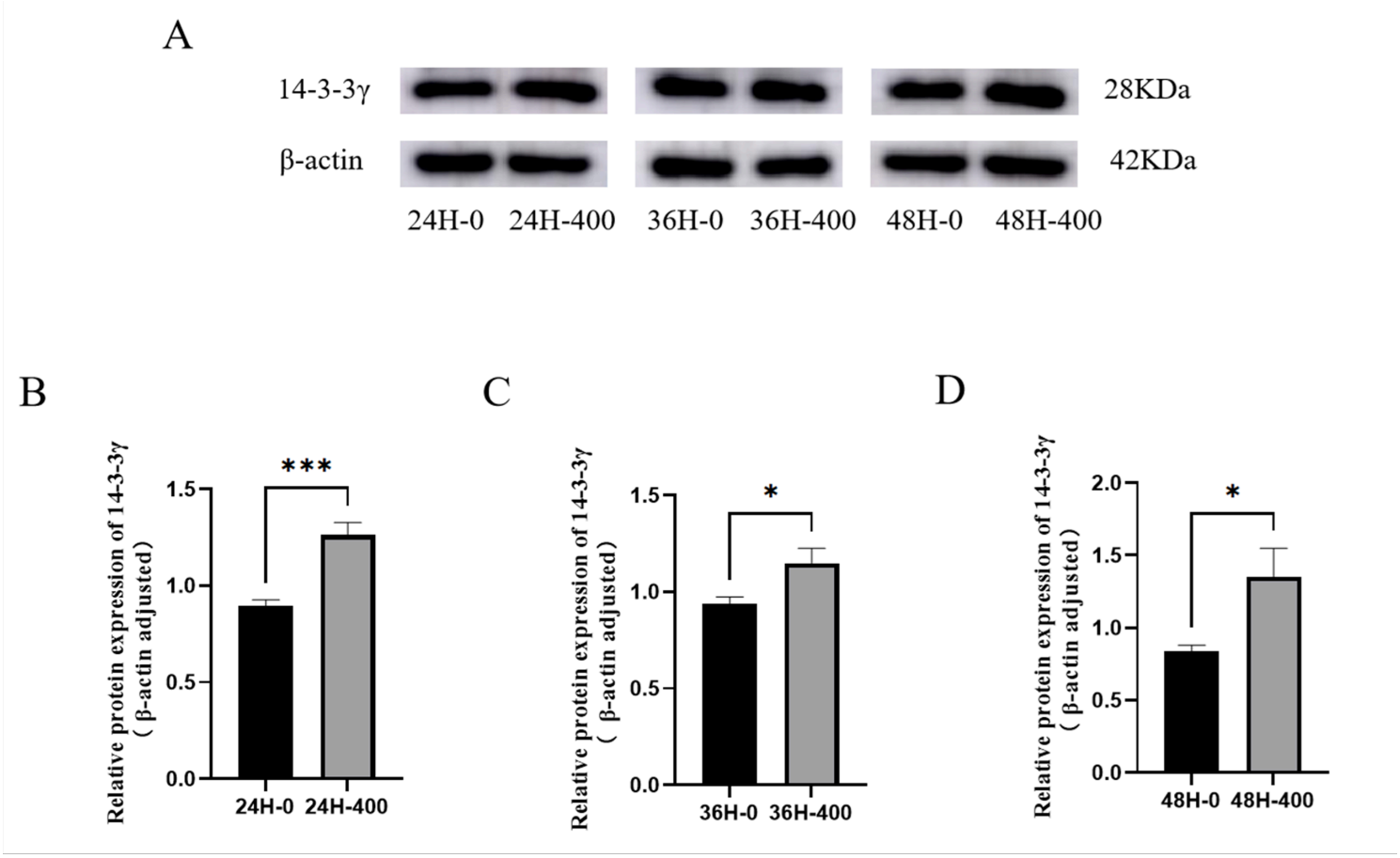


Figure 3

Western blot analysis of 14-3-3γ protein expression after 400 μM $CoCl_2$ treatment for 24, 36 and 48 h.

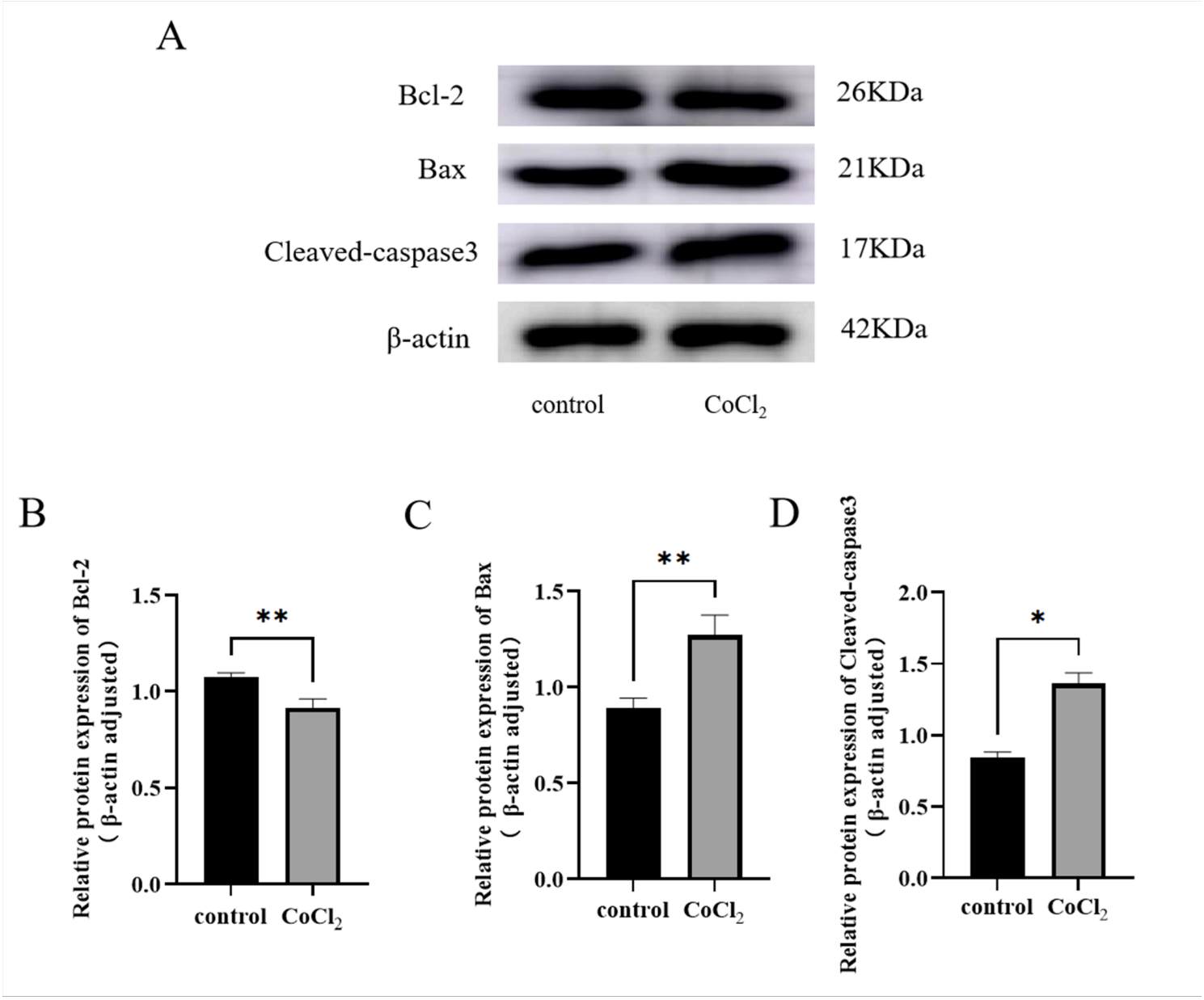


Figure 4

Western blot analysis of Bax, Bcl-2 and cleaved caspase-3 after $CoCl_2$-induced chemical hypoxia-like injury.

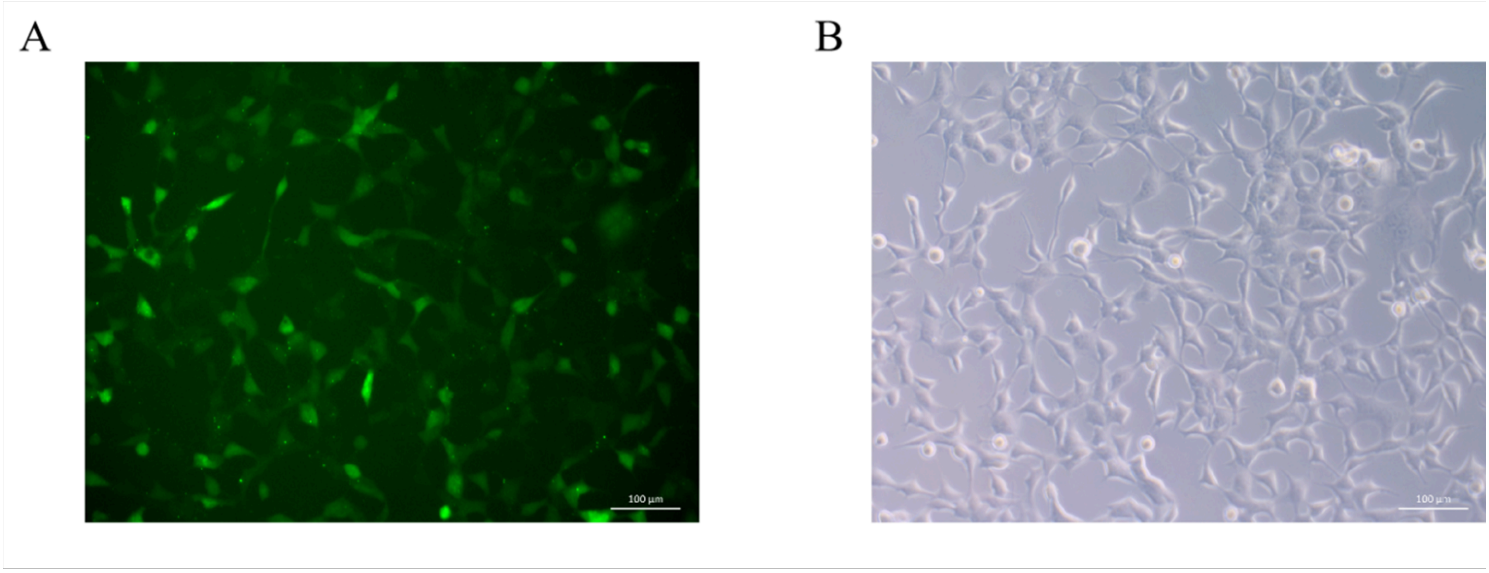


Figure 5

Fluorescence microscopy showing FAM-labeled siRNA transfection in SH-SY5Y cells.

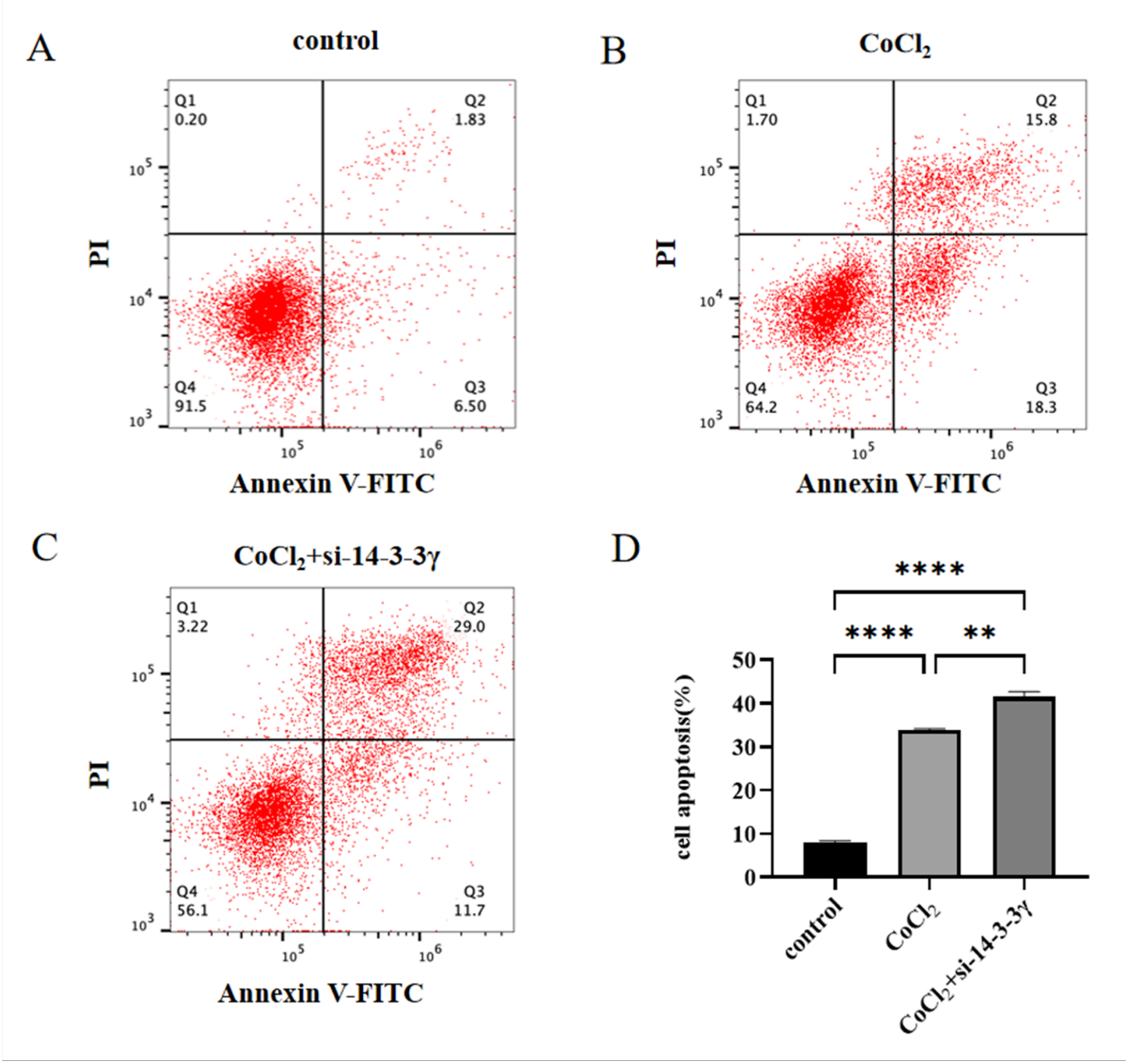


Figure 6

Annexin V-FITC/PI flow cytometry showing that 14-3-3γ knockdown aggravates $CoCl_2$-induced apoptosis.

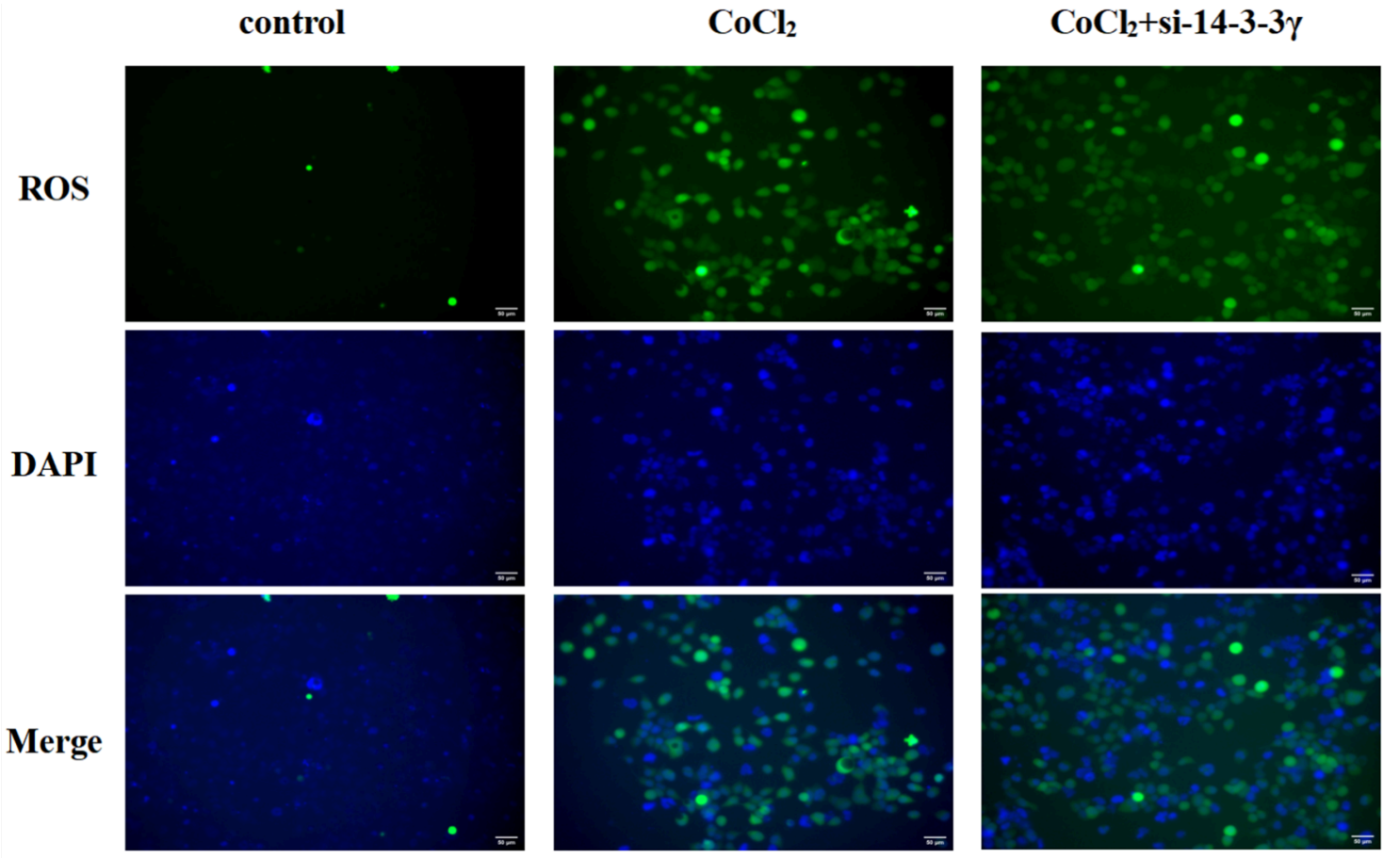


Figure 7

DCFH-DA fluorescence showing that 14-3-3γ knockdown enhances ROS accumulation under $CoCl_2$-induced stress.

Image not available with this version

Figure 8

Western blot analysis showing that 14-3-3γ knockdown increases the Bax/Bcl-2 ratio and cleaved caspase-3 expression under $CoCl_2$-induced stress.